

# LOWER BOUND ON THE COSMIC TEV GAMMA-RAY BACKGROUND RADIATION

YOSHIYUKI INOUE<sup>1</sup>

Institute of Space and Astronautical Science JAXA, 3-1-1 Yoshinodai, Chuo-ku, Sagami-hara, Kanagawa 252-5210, Japan

YASUYUKI T. TANAKA

Hiroshima Astrophysical Science Center, Hiroshima University, 1-3-1 Kagamiyama, Higashi-Hiroshima, Hiroshima 739-8526, Japan  
*Accepted for publication in ApJ*

## ABSTRACT

The *Fermi* gamma-ray space telescope has revolutionized our understanding of the cosmic gamma-ray background radiation in the GeV band. However, investigation on the cosmic TeV gamma-ray background radiation still remains sparse. Here, we report the lower bound on the cosmic TeV gamma-ray background spectrum placed by the cumulative flux of individual detected extragalactic TeV sources including blazars, radio galaxies, and starburst galaxies. The current limit on the cosmic TeV gamma-ray background above 0.1 TeV is obtained as  $2.8 \times 10^{-8} (E/100 \text{ GeV})^{-0.55} \exp(-E/2100 \text{ GeV}) [\text{GeV}/\text{cm}^2/\text{s}/\text{sr}] < E^2 dN/dE < 1.1 \times 10^{-7} (E/100 \text{ GeV})^{-0.49} [\text{GeV}/\text{cm}^2/\text{s}/\text{sr}]$ , where the upper bound is set by requirement that the cascade flux from the cosmic TeV gamma-ray background radiation can not exceed the measured cosmic GeV gamma-ray background spectrum (Inoue & Ioka 2012). Two nearby blazars, Mrk 421 and Mrk 501, explain  $\sim 70\%$  of the cumulative background flux at 0.8–4 TeV, while extreme blazars start to dominate at higher energies. We also provide the cumulative background flux from each population, i.e. blazars, radio galaxies, and starburst galaxies which will be the minimum requirement for their contribution to the cosmic TeV gamma-ray background radiation.

*Subject headings:* gamma rays: diffuse background - gamma rays: general - cosmic background radiation

## 1. INTRODUCTION

The *Fermi* gamma-ray space telescope (hereinafter *Fermi*) has successfully measured the cosmic gamma-ray background (CGB) spectrum at 0.1–820 GeV (Ackermann et al. 2015). The CGB represents superposed gamma-ray flux from all resolved and unresolved gamma-ray sources in the universe outside of the Milky way<sup>2</sup>. In this paper, we simply refer to the total CGB as the CGB otherwise noticed.

Various gamma-ray emitting sources have been discussed as the origins of the CGB in the literature (see Inoue 2014; Fornasa & Sánchez-Conde 2015, for recent reviews). *Fermi* enables us to understand its composition at  $>0.1$  GeV (Ajello et al. 2015; Di Mauro & Donato 2015) as blazars (e.g. Ajello et al. 2012, 2014), radio galaxies (e.g. Inoue 2011a), and star-forming galaxies (e.g. Ackermann et al. 2012). At  $>50$  GeV, source count analysis based on the *Fermi* source catalog detected above 50 GeV (2FHL; The Fermi-LAT Collaboration 2015a) found that current detected populations make up  $86^{+16}_{-14}\%$  of the CGB and its source counts are compatible with the expected blazar source counts (The Fermi-LAT Collaboration 2015b).

The cosmic TeV gamma-ray background, however, has not been well investigated yet. At the TeV energy region, ground based gamma-ray telescopes such as imaging atmospheric Cherenkov telescopes (IACTs) observe gamma rays through

the air shower produced by the gamma ray interacting with the atmosphere. Since hadrons and electrons also produce air shower, those background events need to be subtracted. In the standard analysis procedure, the background flux level is determined using regions of no gamma-ray emitting objects but in the same field of view (Berge et al. 2007). This method subtracts the CGB emission signals together with other hadronic and leptonic backgrounds. It is therefore difficult to measure the isotropic diffuse CGB radiation with this method, although the Galactic diffuse emission has recently been measured by the H.E.S.S. collaboration (Abramowski et al. 2014).

As an aside, the IceCube Collaboration has recently reported detection of several tens of TeV–PeV neutrino events (Aartsen et al. 2013, 2014). The origin of the IceCube neutrinos are still under debate (see e.g. Murase 2015, for reviews). Conventionally, those high energy neutrinos are produced by cosmic rays via hadronuclear ( $pp$ ) and/or photohadronic ( $p\gamma$ ) interactions. In either case, gamma rays are accompanied with. The current unresolved CGB spectrum at the GeV band constrains  $pp$  scenarios as the origin of IceCube TeV–PeV neutrino events (Murase et al. 2013; Bechtol et al. 2015) because a power-law secondary spectrum following the initial cosmic-ray spectrum is generated. As gamma-ray and neutrino spectra of  $p\gamma$  scenarios depend on target photon densities (e.g. Murase et al. 2014; Dermer et al. 2014), spectral extrapolation like the  $pp$  models is not valid. Therefore, the cosmic TeV–PeV gamma-ray background spectrum would be useful to constrain neutrino origins further. However, gamma rays above  $\sim 100$  GeV propagating through the universe experience absorption by the interaction with the extragalactic background light (EBL) via electron–positron pair production (e.g. Gould & Schröder 1966; Jelley 1966; Stecker et al. 1992; Finke et al. 2010; Domínguez et al. 2011; Inoue et al. 2013). This EBL attenuation may severely suppress TeV gamma-ray

yinoue@astro.isas.jaxa.jp

<sup>1</sup> JAXA International Top Young Fellow

<sup>2</sup> The cosmic gamma-ray background (CGB) is also called as the extragalactic gamma-ray background (EGRB or EGB) or the isotropic gamma-ray background (IGRB) where the EGB is the total (resolved and unresolved) CGB and the IGRB is the unresolved CGB (e.g. Ackermann et al. 2015). In other wavelengths, it is common to use the term of the cosmic background radiation such as the cosmic microwave, infrared, optical, and X-ray background radiation.

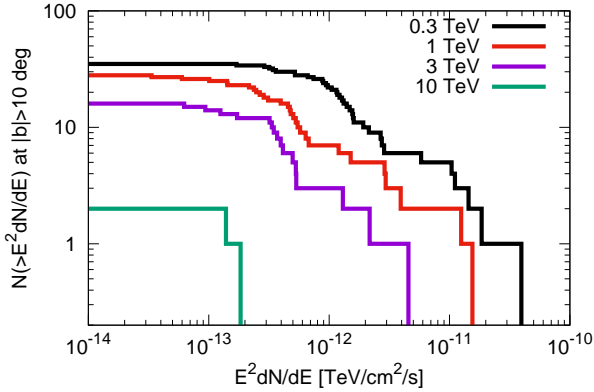


FIG. 1.— Cumulative source count distribution of extragalactic TeV detected objects at  $|b| > 10$  deg as a function of energy flux at an energy indicated in the figure. The sample includes blazars, radio galaxies, and starburst galaxies. Each line corresponds to the distribution at 0.3 TeV, 1 TeV, 3 TeV, and 10 TeV from top to bottom.

signals from neutrino origins, while neutrinos are not suppressed.

In this paper, we place the lower bound on to the cosmic TeV gamma-ray background spectrum. Current IACTs have detected 131 sources (TeVcat; Wakely & Horan 2008)<sup>3</sup> of which  $\sim 50$  sources are extragalactic objects, blazars, radio galaxies, and starburst galaxies. Integration of low-state flux of those extragalactic TeV sources provides a firm lower limit on the cosmic TeV gamma-ray background radiation. This method is an analogy of galaxy counts which integrate the flux of individual detected galaxies and gives a lower bound on to the EBL (e.g. Madau & Pozzetti 2000; Totani et al. 2001). We also show the cumulative flux of each population and the allowed range of the cosmic TeV gamma-ray background radiation together with the upper bound which is placed not to make the GeV cascade component of the cosmic TeV gamma-ray background radiation exceed the measured unresolved CGB spectrum (Inoue & Ioka 2012).

## 2. EXTRAGALACTIC TEV SOURCE SAMPLES

We select 35 known extragalactic TeV sources which are located at Galactic latitude  $|b| > 10$  deg and whose low activity state flux is available, since our aim is to give conservative constraints on the CGB in the TeV band. It is not straightforward to define the low-state flux with IACTs because IACTs do not always monitor sources like *Fermi*. Therefore, for each source, we select the lowest fluxes among several TeV measurements by modern IACTs (H.E.S.S., MAGIC, and VERITAS) and further restrict samples showing no significant variability in the TeV band during observations. The sample contains 30 blazars, 3 radio galaxies, and 2 starburst galaxies from the default TeVcat catalog (Wakely & Horan 2008) which include published sources only. Energy bins of TeV gamma-ray spectra in the literature are different among papers. To make energy bins even, we rebin TeV spectra by interpolating between each binned data in the range of reported energies. We also include the *Fermi* third source (3FGL) catalog data (Acero et al. 2015) to cover GeV gamma-ray spectra. The 3FGL catalog is based on its first 48 months of survey data. All of our sample have counterparts in the 3FGL catalog. Our sample is summarized in Table 1.

<sup>3</sup> <http://tevcat.uchicago.edu/>

Figure 1 shows the cumulative source count distribution of our TeV source sample at 0.3 TeV, 1 TeV, 3 TeV, and 10 TeV. As energy increases, the number of the sample decreases. The apparent distribution at each energy is different from a uniform distribution in the Euclidean universe. However, the sky coverage of current IACTs is not uniform. Further discussion on the cumulative source count distribution at the TeV band requires more uniform and wide sky coverage by future experiments (Inoue et al. 2010) such as the Cherenkov Telescope Array (CTA; Actis et al. 2011) and the High Altitude Water Cherenkov observatory (HAWC; Abeysekara et al. 2013).

## 3. LOWER BOUNDS ON THE COSMIC GAMMA-RAY BACKGROUND RADIATION

The lower bound on the cosmic TeV gamma-ray background is obtained by integrating flux of our TeV samples at each energy bin. To convert this integrated flux to the cumulative background flux, we divide the flux by the sky area above  $|b| \geq 10$  deg ( $\simeq 3.3\pi$  str). The obtained background spectrum at each energy is tabulated in Table 2. The uncertainties at each energy is also estimated by integrating the rebinned 1-sigma upper and lower bounds of each source and by dividing those values by the sky area above  $|b| \geq 10$  deg. Figure 2 shows the lower bound on the cosmic TeV gamma-ray background radiation spectrum together with the *Fermi* CGB spectrum (Ackermann et al. 2015). The TeV CGB flux resolved by current IACTs is dominated by two nearby bright blazars, Mrk 421 and Mrk 501. These two objects make  $\sim 70\%$  of the flux at 0.8–4 TeV. At  $> 4$  TeV, on the other hand, extreme blazars, H1426-428 and 1ES 0229+200, both of which are detected up to  $\sim 10$  TeV start to dominate the background flux.

The obtained lower bound above 100 GeV is well approximated as

$$E^2 \frac{dN}{dE} \geq 2.8^{+0.72}_{-0.63} \times 10^{-8} \left( \frac{E}{100 \text{ GeV}} \right)^{-(0.55^{+0.047}_{-0.020})} \times \exp \left( -\frac{E}{2.1^{+0.80}_{-0.47} \times 10^3 \text{ GeV}} \right) [\text{GeV}/\text{cm}^2/\text{s}/\text{sr}]$$

The exponential cutoff may indicate the feature of gamma-ray attenuation by EBL in the CGB spectrum. However, it can be also interpreted as the intrinsic gamma-ray spectral cutoff in individual gamma-ray sources, since Mrk 421 and Mrk 501 dominate the lower bound and the gamma-ray opacity at the distance to these two blazars becomes unity at  $\sim 7$  TeV (e.g. Inoue et al. 2013).

For the comparison, we also show in Figure 2 the *Fermi* resolved CGB spectrum which corresponds to the cumulative flux of the *Fermi* detected sources in Ackermann et al. (2015). The cumulative flux of the 2FHL catalog sources is also shown. For the 2FHL sources, we collect sources at  $|b| \geq 10$  deg listed in the 2FHL catalog (The Fermi-LAT Collaboration 2015a) where 257 objects are included.

Current IACTs have resolved  $\sim 30\%$  of the CGB flux measured by *Fermi* at  $\sim 1$  TeV, while *Fermi* itself has remarkably resolved  $\sim 90\%$  of that. The resolved fraction is consistent between Ackermann et al. (2015) and the 2FHL catalog (The Fermi-LAT Collaboration 2015a). Although the resolved CGB flux by IACTs is consistent with the *Fermi* resolved CGB flux considering uncertainties, this difference should be addressed because current IACTs have about a factor of 40 better sensitivity at 1 TeV than *Fermi* (see also <http://www.slac.stanford.edu/exp/glast/groups/can> for the latest *Fermi* sensitivity Funk et al. 2013).

TABLE 1  
EXTRAGALACTIC TEV GAMMA-RAY OBJECTS AT  $|b| \geq 10$  DEG

Source	R.A. [deg]	Dec. [deg]	l [deg]	b [deg]	Class	3FGL Name	Reference
SHBL J001355.9-185406	3.48	-18.90	74.63	-78.08	blazar	3FGL J0013.9-1853	Abramowski et al. (2013a)
NGC 253	11.89	-25.27	97.50	-87.95	starburst galaxy	3FGL J0047.5-2516	Abramowski et al. (2012c)
RGB J0152+017	28.16	1.81	152.36	-57.52	blazar	3FGL J0152.6+0148	Aharonian et al. (2008)
3C 66A	35.67	43.03	140.15	-16.77	blazar	3FGL J0222.6+4301	Aleksić et al. (2011)
1ES 0229+200	38.22	20.27	152.97	-36.62	blazar	3FGL J0232.8+2016	Aharonian et al. (2007c)
PKS 0301-243	45.87	-24.12	214.63	-60.17	blazar	3FGL J0303.4-2407	Abramowski et al. (2013b)
NGC 1275	49.96	41.51	150.58	-13.26	radio galaxy	3FGL J0319.8+4130	Aleksić et al. (2014)
RBS 0413	49.97	18.79	165.09	-31.67	blazar	3FGL J0319.8+1847	Aliu et al. (2012)
1ES 0347-121	57.31	-11.98	201.89	-45.74	blazar	3FGL J0349.2-1158	Aharonian et al. (2007b)
1ES 0414+009	64.22	1.08	191.83	-33.16	blazar	3FGL J0416.8+0104	Abramowski et al. (2012a)
PKS 0548-322	87.66	-32.28	237.58	-26.15	blazar	3FGL J0550.6-3217	Aharonian et al. (2010)
RGB J0710+591	107.59	59.15	157.39	25.41	blazar	3FGL J0710.3+5908	Acciari et al. (2010b)
S5 0716+71	110.49	71.35	143.98	28.02	blazar	3FGL J0721.9+7120	Anderhub et al. (2009)
1ES 0806+524	122.45	52.31	166.26	32.91	blazar	3FGL J0809.8+5218	Acciari et al. (2009a)
M 82	148.87	69.67	141.44	40.54	starburst galaxy	3FGL J0955.4+6940	Acciari et al. (2009b)
1RXS J101015.9-311909	152.57	-31.34	266.93	20.04	blazar	3FGL J1010.2-3120	Abramowski et al. (2012b)
1ES 1011+496	153.77	49.43	165.53	52.72	blazar	3FGL J1015.0+4925	Albert et al. (2007b)
1ES 1101-232	165.89	-23.49	273.18	33.08	blazar	3FGL J1103.5-2329	Aharonian et al. (2007a)
Mrk 421	166.12	38.21	179.83	65.03	blazar	3FGL J1104.4+3812	Albert et al. (2007c)
1ES 1215+303	184.46	30.12	188.87	82.05	blazar	3FGL J1217.8+3007	Aleksić et al. (2012b)
1ES 1218+304	185.34	30.18	186.36	82.73	blazar	3FGL J1221.3+3010	Acciari et al. (2009c)
M 87	187.73	12.41	283.84	74.51	radio galaxy	3FGL J1230.9+1224	Aleksić et al. (2012c)
1ES 1312-423	198.69	-42.63	307.50	20.04	blazar	3FGL J1314.7-4237	Abramowski et al. (2013c)
Cen A	201.37	-43.03	309.52	19.41	radio galaxy	3FGL J1325.4-4301	Aharonian et al. (2009)
PKS 1424+240	216.76	23.80	29.49	68.20	blazar	3FGL J1427.0+2347	Acciari et al. (2010a)
H 1426+428	217.15	42.67	77.47	64.89	blazar	3FGL J1428.5+4240	Aharonian et al. (2002)
AP Librae	229.42	-24.38	340.68	27.58	blazar	3FGL J1517.6-2422	Abramowski et al. (2015)
PG 1553+113	238.94	11.19	21.92	43.96	blazar	3FGL J1555.7+1111	Aleksić et al. (2012d)
Mrk 501	253.48	39.75	63.59	38.85	blazar	3FGL J1653.9+3945	Albert et al. (2007d)
1ES 1959+650	300.02	65.15	98.01	17.67	blazar	3FGL J2000.0+6509	Albert et al. (2006)
PKS 2005-489	302.35	-48.83	350.38	-32.60	blazar	3FGL J2009.3-4849	Acero et al. (2010)
PKS 2155-304	329.72	-30.23	17.73	-52.25	blazar	3FGL J2158.8-3013	Abramowski et al. (2010)
BL Lac	330.69	42.28	92.60	-10.44	blazar	3FGL J2202.7+4217	Albert et al. (2007a)
B3 2247+381	342.53	38.42	98.26	-18.57	blazar	3FGL J2250.1+3825	Aleksić et al. (2012a)
H 2356-309	359.83	-30.65	12.71	-78.07	blazar	3FGL J2359.3-3038	Aharonian et al. (2006)

TABLE 2  
THE LOWER BOUND ON THE COSMIC TEV GAMMA-RAY BACKGROUND SPECTRUM

Energy (GeV)	Lower Bound Spectrum $E^2 dN/dE$ (GeV/cm <sup>2</sup> /s/sr)
0.20	$(1.9 \pm 0.2) \times 10^{-8}$
0.65	$(2.0 \pm 0.1) \times 10^{-8}$
2.0	$(2.1 \pm 0.1) \times 10^{-8}$
6.5	$(2.3 \pm 0.1) \times 10^{-8}$
55	$(2.5 \pm 0.2) \times 10^{-8}$
130	$(2.3^{+0.6}_{-0.5}) \times 10^{-8}$
205	$(1.9 \pm 0.5) \times 10^{-8}$
325	$(1.2 \pm 0.3) \times 10^{-8}$
515	$(9.0^{+2.0}_{-2.3}) \times 10^{-9}$
815	$(6.1 \pm 1.8) \times 10^{-9}$
1300	$(3.4^{+1.2}_{-0.9}) \times 10^{-9}$
2050	$(2.1^{+0.8}_{-0.6}) \times 10^{-9}$
3250	$(1.2^{+0.5}_{-0.4}) \times 10^{-9}$
5150	$(9.6^{+3.7}_{-2.9}) \times 10^{-10}$
8200	$(3.1^{+6.4}_{-2.5}) \times 10^{-11}$
13000	$(3.1^{+6.4}_{-2.5}) \times 10^{-11}$

The difference of resolved fractions may be due to the sky coverage difference. *Fermi* covers the whole sky, while current IACTs cover only limited sky regions. In the 2FHL catalog,  $\sim 78\%$  of the sources which are detected at  $> 50$  GeV are not observed by IACTs. However, only 14 objects are listed at the highest energy bin (585–2000 GeV) at  $|b| \geq 10$  deg in the 2FHL catalog and our sample includes 30 sources at energies above 585 GeV. Therefore, the difference of the sky coverages might not be the main cause of this resolved fraction difference. This implies a few bright objects dominate

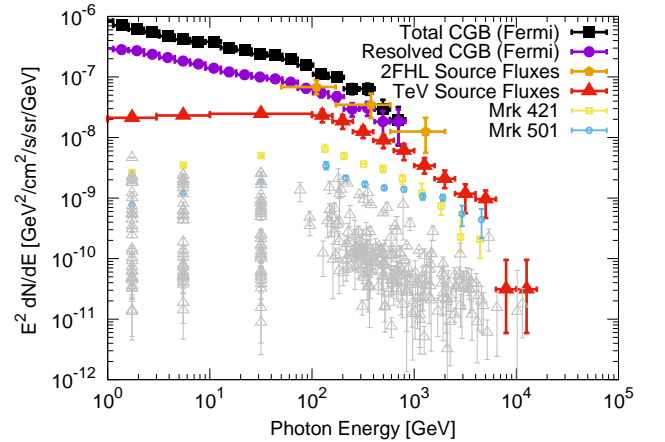


FIG. 2.— The cosmic gamma-ray background spectrum at the GeV–TeV band. The lower bound on the cosmic TeV gamma-ray background obtained from the cumulative flux of 35 known extragalactic TeV objects at  $|b| > 10$  deg is shown by filled triangles. Filled square, filled circle, and filled pentagon data points represent the total CGB spectrum measured by *Fermi* (Ackermann et al. 2015), the resolved CGB spectrum by *Fermi* (Ackermann et al. 2015), and the cumulative 2FHL extragalactic source fluxes based on The Fermi-LAT Collaboration (2015a). The contributions of individual objects are shown by open triangle data, where the flux is divided by the sky area at  $|b| > 10$  deg. Open square and circle points represent that of Mrk 421 and Mrk 501, respectively. The error bars correspond to 1- $\sigma$  uncertainty.

the cosmic TeV gamma-ray background flux as the resolved component is dominated by Mrk 421 and Mrk 501.

Another interpretation is temporal variability. The CGB



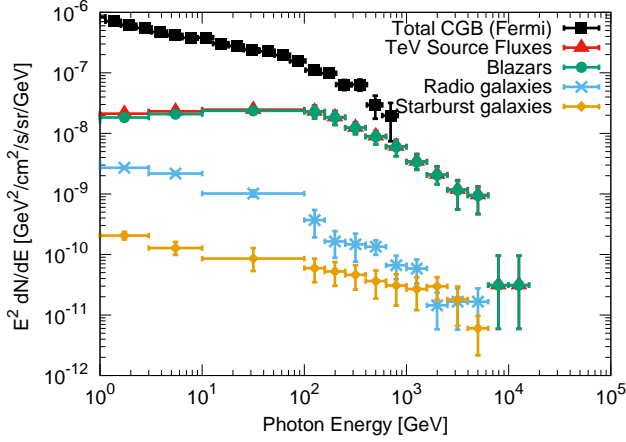


FIG. 3.— Cumulative gamma-ray background spectrum from various populations detected in the TeV band. Circle, cross, and diamond points correspond to cumulative flux of detected blazars, radio galaxies, and starburst galaxies at  $|b| > 10$  deg, respectively. The lower bound of the cosmic TeV gamma-ray background from the cumulative flux of those populations is shown by triangle. Square data points represent the total CGB spectrum measured by *Fermi* (Ackermann et al. 2015). The error bars correspond to  $1\text{-}\sigma$  uncertainty. As the TeV source counts are dominated by blazars, circle and triangle points almost overlap each other.

spectrum is the time-averaged spectrum of all over the sky taken by the first 50 months operation of the *Fermi*. The 2FHL catalog averages the source variation in 80 months of data. As blazars are highly variable (e.g. Abdo et al. 2010), average flux is expected to be higher than low-state flux. For example, the gamma-ray flux of Mrk 421 at 585–2000 GeV is  $5.1^{+1.6}_{-1.3} \times 10^{-11}$  ph/cm<sup>2</sup>/s and  $1.9^{+0.50}_{-0.37} \times 10^{-11}$  ph/cm<sup>2</sup>/s in the 2FHL catalog and our sample data (Albert et al. 2007c), respectively. Since we have collected low-state data only to put a conservative lower bound on the cosmic TeV gamma-ray background radiation, the obtained bound can be lower than the averaged 2FHL and *Fermi* resolved CGB flux. This flux difference of Mrk 421 alone would reconcile the difference between the 2FHL source flux and the IACTs source flux.

The gamma-ray flux of the other dominant blazar Mrk 501 at 585–2000 GeV is  $1.1^{+0.75}_{-0.51} \times 10^{-11}$  ph/cm<sup>2</sup>/s and  $1.5^{+0.17}_{-0.16} \times 10^{-11}$  ph/cm<sup>2</sup>/s in the 2FHL catalog and our sample data (Albert et al. 2007d), respectively, which are relatively similar to each other. It is known that Mrk 421 shows more frequent variabilities than Mrk 501 (Abdo et al. 2011a,b). Continuous monitoring and understanding of duty cycle of extragalactic gamma-ray sources especially Mrk 421 are necessary to obtain the averaged gamma-ray flux and the resolved CGB flux.

Figure 3 shows the cumulative TeV gamma-ray spectrum from each population; blazars, radio galaxies, and starburst galaxies. As 30 of 35 samples are blazars, they dominate the cumulative flux of currently known extragalactic TeV sources. In the GeV band, it is well-known that blazars dominate the cosmic gamma-ray background radiation (e.g. Inoue & Totani 2009; Ajello et al. 2012, 2014, 2015; Di Mauro & Donato 2015), while radio galaxies (e.g. Inoue 2011a; Di Mauro et al. 2014) and starburst galaxies (e.g. Pavlidou & Fields 2002; Fields et al. 2010; Makiya et al. 2011; Ackermann et al. 2012; Lacki et al. 2014) make sub-dominant contributions. The contribution of radio galaxies and starburst galaxies is approximated by a power-law spectral shape with an index of  $-0.9$  and  $-0.5$  in  $E^2 dN/dE$ , respectively.

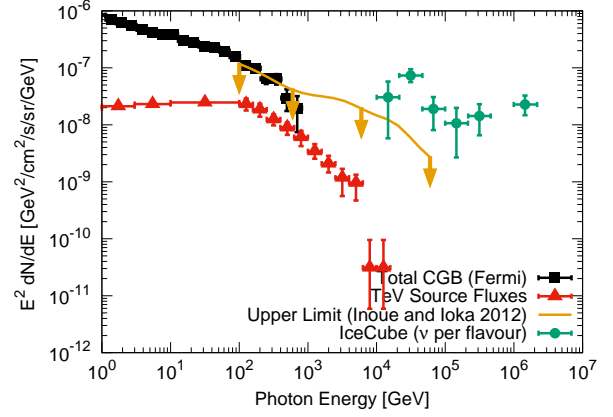


FIG. 4.— The cosmic background photon and neutrino spectra from GeV to PeV. The square, triangle, and circle data points represent the total CGB spectrum measured by *Fermi* (Ackermann et al. 2015), the cumulative flux of known extragalactic TeV objects at  $|b| > 10$  deg (the lower bound), and the IceCube neutrino flux per flavour (Aartsen et al. 2014), respectively. The solid curve with arrows represents the upper bound on the CGB requiring cascade emission not to exceed the EGB data below 100 GeV in the model-independent way (Inoue & Ioka 2012). Error bars correspond to  $1\text{-}\sigma$  uncertainty of data.

#### 4. DISCUSSION AND CONCLUSION

In this paper, we obtain the lower bound on the cosmic TeV gamma-ray background spectrum. The bound is set by the cumulative flux of known TeV gamma-ray objects at  $|b| \geq 10$  deg. We collect low-state flux data of 35 TeV gamma-ray emitting objects. By including the 3FGL data catalog, the bounds is set from 100 MeV to  $\sim 10$  TeV. The bound is dominated by two nearby blazars Mrk 421 and Mrk 501 which make  $\sim 70\%$  of the resolved CGB by IACTs at  $\sim 0.8\text{--}4$  TeV. However, at higher energies, extreme blazars which are more distant than Mrk 421 and Mrk 501 start to dominate. Comparing with the CGB spectrum measured by *Fermi*, current known TeV sources explain  $\sim 30\%$  of the *Fermi* CGB flux at  $\sim 1$  TeV.

Here, EBL photons attenuate gamma rays through the electron–positron pair production process. Those pairs scatter the cosmic microwave background (CMB) radiation via the inverse Compton scattering and generate secondary gamma-ray emission component (the so-called cascade emission; e.g. Protheroe 1986; Aharonian et al. 1994; Fan et al. 2004).<sup>4</sup> The cascade component must contribute to the cosmic GeV gamma-ray background radiation, if there is the cosmic TeV gamma-ray background radiation (Coppi & Aharonian 1997; Murase et al. 2012a; Inoue & Ioka 2012; Ackermann et al. 2015). The level of the upper bound weakly depends on the assumed spectral energy distribution and evolution of contributors to be consistent with the *Fermi* measurements (Inoue & Ioka 2012). By setting no evolution, a power-law emission with a photon index of 1.5, and a cutoff energy of 60 TeV, the current unresolved CGB measurement below 100 GeV sets an upper bound on the CGB itself at  $> 100$  GeV as  $1.1 \times 10^{-7} (E/100 \text{ GeV})^{-0.49}$  GeV/cm<sup>2</sup>/s/sr (Inoue & Ioka 2012).

Combining with the lower and upper bounds, the allowed range of the cosmic TeV gamma-ray

<sup>4</sup> Although plasma beam instability may suppress the cascade emission (Broderick et al. 2012), recent Particle-In-Cell simulations reveals that the plasma instability carries 10% of the attenuated energy at most (Sironi & Giannios 2014).

background spectrum is approximated as  $2.8 \times 10^{-8}(E/100 \text{ GeV})^{-0.55} \exp(-E/2100 \text{ GeV}) [\text{GeV}/\text{cm}^2/\text{s}/\text{sr}] < E^2 dN/dE < 1.1 \times 10^{-7}(E/100 \text{ GeV})^{-0.49} [\text{GeV}/\text{cm}^2/\text{s}/\text{sr}]$ . Figure 4 shows the current bounds on the cosmic TeV gamma-ray background radiation together with the IceCube neutrino flux per flavour (Aartsen et al. 2014). As the current *Fermi* unresolved CGB measurements give constraints on the origin of the TeV-PeV neutrino background (e.g. Murase et al. (2013); Bechtol et al. (2015)), but see also Murase et al. (2015); Kistler (2015)), our bounds at the TeV band may be useful for the further constraints. However, it should be noted that gamma-ray attenuation by the EBL photons suppresses the associated gamma-ray signals (e.g. Finke et al. 2010; Domínguez et al. 2011; Inoue et al. 2013; Khaire & Srianand 2015), while neutrinos are not suppressed. Moreover, if neutrinos and gamma rays are generated in dense environments like starforming galaxies, TeV gamma rays can be internally attenuated by pair production because of luminous interstellar radiation photon field (e.g. Domingo-Santamaría & Torres 2005; Inoue 2011b; Murase 2015; Kistler 2015).

Next generation ground gamma-ray telescopes CTA will have a factor of  $\sim 10$  better sensitivity than current IACTs (Actis et al. 2011). And, HAWC which covers over 5 str of the sky will achieve better sensitivity and wider energy coverage than current IACTs do (Abeysekara et al. 2013). Once these observatories perform extragalactic surveys, more TeV sources are expected to be detected (Inoue et al. 2010; Dubus et al. 2013). Future CTA and HAWC sky surveys will tighten the current lower bound further. If the cosmic TeV gamma-ray background flux is close to our lower bound and dominated by a few objects as our results show, strong anisotropy signature can be expected.

At  $\gtrsim 10$  TeV, the lower bound on the cosmic TeV gamma-ray background seems to be flat in  $E^2 dN/dE$ , although the flux uncertainty is still large. At these energy band, extreme blazars make up the cumulative flux rather than nearby bright blazars. Extreme blazars do not show apparent variabilities

and hard gamma-ray spectra and the one-zone synchrotron self-Compton model fits requires extreme parameters (see Tanaka et al. 2014, and references therein). Various models have been proposed to explain extreme blazars such as the stochastic acceleration scenarios (Lefa et al. 2011) and the lepto-hadronic emission scenario (Cerruti et al. 2015). Exotic scenarios are also discussed such as hypothetical axion-like particles (de Angelis et al. 2007; Simet et al. 2008; Sánchez-Conde et al. 2009), as well as Lorentz invariance violation (Kifune 1999; Protheroe & Meyer 2000).

An alternative interpretation for extreme blazars is the cascade emission from high energy cosmic rays propagating through intergalactic space. Protons or neutrons escaping from the jet initiate cascades with EBL or CMB (e.g. Essey & Kusenko 2010; Murase et al. 2012b; Takami et al. 2013; Essey & Kusenko 2014). In the cascade scenario, the observed fluxes contain two emission components: primary gamma-ray flux produced at the source and secondary gamma-ray flux, which arises from line-of-sight interactions of cosmic rays during the propagation. A secondary gamma-ray component from the cascade scenario creates a flat spectrum above several TeV to a few tens of TeV. Despite EBL attenuation, the cascade scenarios allow us to detect many blazars even at  $> 1$  TeV beyond the EBL attenuation horizon (Inoue et al. 2014). Flat signature in the cosmic TeV gamma-ray background radiation will be a key for the test of the cosmic-ray induced cascade scenario and for the understanding of neutrino origins as this cascade process also produces TeV-PeV neutrinos (Essey et al. 2011; Kalashev et al. 2013).

The authors thank the anonymous referee for useful comments and suggestions. The authors would also like to thank Marco Ajello, John Beacom, and Mattia Di Mauro for useful comments and discussions. Y.I. acknowledges support by the JAXA international top young fellowship. YTT is supported by Kakenhi 15K17652.

## REFERENCES

- Aartsen, M. G. et al. 2013, *Physical Review Letters*, 111, 021103 [1]  
Aartsen, M. G. et al. 2014, *Physical Review Letters*, 113, 101101 [1, 4]  
Abdo, A. A. et al. 2010, *ApJ*, 722, 520 [3]  
Abdo, A. A. et al. 2011a, *ApJ*, 736, 131 [3]  
Abdo, A. A. et al. 2011b, *ApJ*, 727, 129 [3]  
Abeysekara, A. U. et al. 2013, *Astroparticle Physics*, 50, 26 [2, 4]  
Abramowski, A. et al. 2010, *A&A*, 520, A83 [1]  
Abramowski, A. et al. 2012a, *A&A*, 538, A103 [1]  
Abramowski, A. et al. 2012b, *A&A*, 542, A94 [1]  
Abramowski, A. et al. 2012c, *ApJ*, 757, 158 [1]  
Abramowski, A. et al. 2013a, *A&A*, 554, A72 [1]  
Abramowski, A. et al. 2013b, *A&A*, 559, A136 [1]  
Abramowski, A. et al. 2013c, *MNRAS*, 434, 1889 [1]  
Abramowski, A. et al. 2014, *Phys. Rev. D*, 90, 122007 [1]  
Abramowski, A. et al. 2015, *A&A*, 573, A31 [1]  
Acciari, V. et al. 2009a, *ApJ*, 690, L126 [1]  
Acciari, V. A. et al. 2009b, *Nature*, 462, 770 [1]  
Acciari, V. A. et al. 2009c, *ApJ*, 695, 1370 [1]  
Acciari, V. A. et al. 2010a, *ApJ*, 708, L100 [1]  
Acciari, V. A. et al. 2010b, *ApJ*, 715, L49 [1]  
Acero, F. et al. 2010, *A&A*, 511, A52 [1]  
Acero, F. et al. 2015, *ApJS*, 218, 23 [2]  
Ackermann, M. et al. 2012, *ApJ*, 755, 164 [1, 3]  
Ackermann, M. et al. 2015, *ApJ*, 799, 86 [1, 2, 3, 3, 2, 3, 4]  
Actis, M. et al. 2011, *Experimental Astronomy*, 32, 193 [2, 4]  
Aharonian, F. et al. 2002, *A&A*, 384, L23 [1]  
Aharonian, F. et al. 2006, *A&A*, 455, 461 [1]  
Aharonian, F. et al. 2007a, *A&A*, 470, 475 [1]  
Aharonian, F. et al. 2007b, *A&A*, 473, L25 [1]  
Aharonian, F. et al. 2007c, *A&A*, 475, L9 [1]  
Aharonian, F. et al. 2008, *A&A*, 481, L103 [1]  
Aharonian, F. et al. 2009, *ApJ*, 695, L40 [1]  
Aharonian, F. et al. 2010, *A&A*, 521, A69 [1]  
Aharonian, F. A., Coppi, P. S., & Voelk, H. J. 1994, *ApJ*, 423, L5 [4]  
Ajello, M. et al. 2012, *ApJ*, 751, 108 [1, 3]  
Ajello, M. et al. 2014, *ApJ*, 780, 73 [1, 3]  
Ajello, M. et al. 2015, *ApJ*, 800, L27 [1, 3]  
Albert, J. et al. 2006, *ApJ*, 639, 761 [1]  
Albert, J. et al. 2007a, *ApJ*, 666, L17 [1]  
Albert, J. et al. 2007b, *ApJ*, 667, L21 [1]  
Albert, J. et al. 2007c, *ApJ*, 663, 125 [1, 3]  
Albert, J. et al. 2007d, *ApJ*, 669, 862 [1, 3]  
Aleksić, J. et al. 2011, *ApJ*, 726, 58 [1]  
Aleksić, J. et al. 2012a, *A&A*, 539, A118 [1]  
Aleksić, J. et al. 2012b, *A&A*, 544, A142 [1]  
Aleksić, J. et al. 2012c, *A&A*, 544, A96 [1]  
Aleksić, J. et al. 2012d, *ApJ*, 748, 46 [1]  
Aleksić, J. et al. 2014, *A&A*, 564, A5 [1]  
Aliu, E. et al. 2012, *ApJ*, 750, 94 [1]  
Anderhub, H. et al. 2009, *ApJ*, 704, L129 [1]  
Bechtol, K., Ahlers, M., Di Mauro, M., Ajello, M., & Vandenbroucke, J. 2015, *arXiv:1511.00688* [1, 4]  
Berge, D., Funk, S., & Hinton, J. 2007, *A&A*, 466, 1219 [1]  
Broderick, A. E., Chang, P., & Pfrommer, C. 2012, *ApJ*, 752, 22 [4]  
Cerruti, M., Zech, A., Boisson, C., & Inoue, S. 2015, *MNRAS*, 448, 910 [4]  
Coppi, P. S. & Aharonian, F. A. 1997, *ApJ*, 487, L9 [4]  
de Angelis, A., Roncadelli, M., & Mansutti, O. 2007, *Phys. Rev. D*, 76, 121301 [4]

- Dermer, C. D., Murase, K., & Inoue, Y. 2014, *Journal of High Energy Astrophysics*, 3, 29 [1]
- Di Mauro, M., Calore, F., Donato, F., Ajello, M., & Latronico, L. 2014, *ApJ*, 780, 161 [3]
- Di Mauro, M. & Donato, F. 2015, *Phys. Rev. D*, 91, 123001 [1, 3]
- Domingo-Santamaría, E. & Torres, D. F. 2005, *A&A*, 444, 403 [4]
- Domínguez, A. et al. 2011, *MNRAS*, 410, 2556 [1, 4]
- Dubus, G. et al. 2013, *Astroparticle Physics*, 43, 317 [4]
- Essey, W., Kalashev, O., Kusenko, A., & Beacom, J. F. 2011, *ApJ*, 731, 51 [4]
- Essey, W. & Kusenko, A. 2010, *Astroparticle Physics*, 33, 81 [4]
- Essey, W. & Kusenko, A. 2014, *Astroparticle Physics*, 57, 30 [4]
- Fan, Y. Z., Dai, Z. G., & Wei, D. M. 2004, *A&A*, 415, 483 [4]
- Fields, B. D., Pavlidou, V., & Prodanović, T. 2010, *ApJ*, 722, L199 [3]
- Finke, J. D., Razzaque, S., & Dermer, C. D. 2010, *ApJ*, 712, 238 [1, 4]
- Fornasa, M. & Sánchez-Conde, M. A. 2015, *Phys. Rep.*, 598, 1 [1]
- Funk, S., Hinton, J. A., & CTA Consortium. 2013, *Astroparticle Physics*, 43, 348 [3]
- Gould, R. J. & Schröder, G. 1966, *Physical Review Letters*, 16, 252 [1]
- Inoue, Y. 2011a, *ApJ*, 733, 66 [1, 3]
- Inoue, Y. 2011b, *ApJ*, 728, 11 [4]
- Inoue, Y. 2014, arXiv:1412.3886 [1]
- Inoue, Y., Inoue, S., Kobayashi, M. A. R., Makiya, R., Niino, Y., & Totani, T. 2013, *ApJ*, 768, 197 [1, 3, 4]
- Inoue, Y. & Ioka, K. 2012, *Phys. Rev. D*, 86, 023003 [(document), 1, 4]
- Inoue, Y., Kalashev, O. E., & Kusenko, A. 2014, *Astroparticle Physics*, 54, 118 [4]
- Inoue, Y. & Totani, T. 2009, *ApJ*, 702, 523 [3]
- Inoue, Y., Totani, T., & Mori, M. 2010, *PASJ*, 62, 1005 [2, 4]
- Jelley, J. V. 1966, *Physical Review Letters*, 16, 479 [1]
- Kalashev, O. E., Kusenko, A., & Essey, W. 2013, *Physical Review Letters*, 111, 041103 [4]
- Kifune, T. 1999, *ApJ*, 518, L21 [4]
- Kistler, M. D. 2015, arXiv:1511.01530 [4]
- Lacki, B. C., Horiuchi, S., & Beacom, J. F. 2014, *ApJ*, 786, 40 [3]
- Lefa, E., Rieger, F. M., & Aharonian, F. 2011, *ApJ*, 740, 64 [4]
- Madau, P. & Pozzetti, L. 2000, *MNRAS*, 312, L9 [1]
- Makiya, R., Totani, T., & Kobayashi, M. A. R. 2011, *ApJ*, 728, 158 [3]
- Murase, K. 2015, in *American Institute of Physics Conference Series*, Vol. 1666, American Institute of Physics Conference Series, 040006 [1, 4]
- Murase, K., Guetta, D., & Ahlers, M. 2015, arXiv:1509.00805 [4]
- Murase, K., Ahlers, M., & Lacki, B. C. 2013, *Phys. Rev. D*, 88, 121301 [1, 4]
- Murase, K., Beacom, J. F., & Takami, H. 2012a, *JCAP*, 8, 30 [4]
- Murase, K., Dermer, C. D., Takami, H., & Migliori, G. 2012b, *ApJ*, 749, 63 [4]
- Murase, K., Inoue, Y., & Dermer, C. D. 2014, *Phys. Rev. D*, 90, 023007 [1]
- Pavlidou, V. & Fields, B. D. 2002, *ApJ*, 575, L5 [3]
- Protheroe, R. J. 1986, *MNRAS*, 221, 769 [4]
- Protheroe, R. J. & Meyer, H. 2000, *Physics Letters B*, 493, 1 [4]
- Sánchez-Conde, M. A., Paneque, D., Bloom, E., Prada, F., & Domínguez, A. 2009, *Phys. Rev. D*, 79, 123511 [4]
- Simet, M., Hooper, D., & Serpico, P. D. 2008, *Phys. Rev. D*, 77, 063001 [4]
- Sironi, L. & Giannios, D. 2014, *ApJ*, 787, 49 [4]
- Stecker, F. W., de Jager, O. C., & Salamon, M. H. 1992, *ApJ*, 390, L49 [1]
- Takami, H., Murase, K., & Dermer, C. D. 2013, *ApJ*, 771, L32 [4]
- Tanaka, Y. T. et al. 2014, *ApJ*, 787, 155 [4]
- The Fermi-LAT Collaboration. 2015a, arXiv:1508.04449 [1, 3, 2]
- The Fermi-LAT Collaboration. 2015b, arXiv:1511.00693 [1]
- Totani, T., Yoshii, Y., Iwamuro, F., Maihara, T., & Motohara, K. 2001, *ApJ*, 550, L137 [1]
- Khaire, V., & Srikanand, R. 2015, *ApJ*, 805, 33 [4]
- Wakely, S. P. & Horan, D. 2008, *International Cosmic Ray Conference*, 3, 1341 [1, 2]